JOURNAL OF MATERIALS SCIENCE **34** (1999) 1353–1365

Diamond deposition on copper: studies on nucleation, growth, and adhesion behaviours

Q. H. FAN*, E. PEREIRA
Department of Physics, University of Aveiro, 3810 Aveiro, Portugal
E-mail: FAN@FIS.UA.PT

J. GRÁCIO
Department of Mechanical Engineering, University of Aveiro, 3810 Aveiro, Portugal

This paper presents a systematic study on diamond growth on copper by microwave plasma chemical vapour deposition (MPCVD). It includes the following four main parts. 1. Effect of substrate pre-treatment on diamond nucleation. 2. Effect of deposition conditions on diamond nucleation and growth. 3. Preparation of free-standing diamond films using copper substrate. 4. Adherent diamond coating on copper using an interlayer. In the first part we show that diamond nucleation on copper is strongly affected by the substrate pre-treatment. The residues of abrasives left in the surface of the copper substrate play an important role in the diamond nucleation. In the second part we show that the diamond growth rate increases with microwave power and gas pressure. The effect of the microwave power is mainly an effect of substrate temperature. Increasing methane concentration results in a higher nucleation density and higher growth rate, but at the cost of a lower film quality. Gas flow rate has little influence on the diamond nucleation density and growth rate. In the third part we demonstrate the possibility of preparing large area free-standing diamond films using copper substrate, which has nearly no carbon affinity and usually leads to weak adhesion of the diamond films. The normally observed film cracking phenomenon is discussed and a two-step growth method is proposed for stress release. In the fourth part we show that adherent diamond coating on copper can be obtained using a titanium interlayer. Residual stress in the films is evaluated by Raman spectroscopy. It is found that with increase in the film thickness, the diamond Raman line shifts from higher wave numbers to lower, approaching 1332 cm^{-1}. The stress variation along the depth of the film is also analysed using Airy stress theory.

1. Introduction

Diamond growth on copper is an interesting topic in both practical and theoretical research. This is because, first, copper is one of the most common and widely used materials in today's industry. If diamond could be deposited on it, there would be many potential applications due to the extreme mechanical, thermal, optical, and electrical properties of diamond. For example, diamond coating on copper may find applications where good thermal conductivity as well as electrical insulation is required. Secondly, like diamond, copper possesses a cubic structure and its lattice parameter is similar to that of diamond (diamond $a = 3.567$ Å, Cu $a = 3.608$ Å). Therefore, in heteroepitaxial growth of diamond on copper the lattice mismatch can be small. Furthermore, copper is a material that has almost no carbon affinity. Diamond growth on copper may present aspects that differ from the mechanism of diamond growth on carbide forming materials such as silicon, which is the most common substrate used for CVD diamond so far. Thus, investigation of diamond growth on copper enables us to understand better the diamond nucleation mechanism, which is still not very clear, as well as to compare the growth characteristics on different kinds of substrate materials.

The fact that copper does not form carbide usually results in weak adhesion of the diamond film, as there is no necessary "glue" at the diamond and copper interface [1]. If free-standing diamond films are desired, this can be an advantage. At present the common method to prepare free-standing diamond film is, first, to deposit the film on substrates like Si, Mo, and Ta, which are carbide forming materials. Then the film is separated from the substrate by chemical etching or mechanical peeling. If relatively pure and uniform diamond films are required, it is necessary to eliminate the interfacial carbide layer between the substrate and the diamond film. In this sense, it is significant to use substrates with

* Author to whom all correspondence should be adressed.

almost no carbon solubility and reaction. This makes copper a promising candidate for direct preparation of high quality free-standing diamond films and we show this possibility in this paper. On the other hand, many applications may require good adhesion of diamond coating on copper. In these cases, the non-carbon affinity of copper appears a disadvantage. To overcome this problem, Narayan *et al*. have showed that good adhesion can be achieved by pulsed laser irradiating and melting the copper surface so that the diamond particles can be embedded into the substrate [2]. In this paper, we demonstrate that adherent diamond coating on copper can also be obtained by using a titanium interlayer.

Actually, one of the main obstacles that hinders diamond growth on copper is that thermally induced stress in the diamond film may be very large due to the large difference in thermal expansion between diamond and copper (at room temperature $\alpha_{\text{diamond}} \approx 1 \times 10^{-6}$/K, $\alpha_{\text{Cu}} \approx 17.6 \times 10^{-6}$/K). This thermal stress influences the adhesion in a negative way and usually causes film cracking during the post-cooling procedure after deposition. So, to avoid film cracking, the thermal stress must be released or reduced, especially when preparing thin, free-standing films. Probably due to this difficulty, so far, there are only a few reports on diamond growth on copper [2–10]. No systematic reports are given on the basic growth characteristics, such as the nucleation behaviour, effect of deposition conditions on the film growth, synthesis of large area diamond film using copper substrate, and adherent diamond coating on copper.

In this paper we present a detailed study on diamond growth on copper. In order to control the diamond nucleation and growth, we first investigate the substrate pre-treatment effect on diamond nucleation. Then the deposition parameter effect on diamond nucleation and growth is studied. On the base of these investigations, free-standing diamond films are prepared using copper substrates. A two-step growth method is proposed to overcome the film cracking problem. Finally, we show that adherent diamond coating on copper can be obtained by using a titanium interlayer. Residual stress in the diamond films is analysed.

2. Experimental

Polycrystalline copper foil (>99.9%) 1 mm thick was used as substrate if not otherwise indicated. Diamond synthesis was conducted using an ASTeX PDS18, 2.45 GHz MPCVD system. A cooled sample stage was installed in this system. The process gases were H_2, CH_4 and O_2. The substrate was put on a Mo sample holder that was placed on the sample stage. The substrate pre-treatment included polishing with SiC sand papers, polishing on fine cloth with diamond pastes, diamond powders, Al_2O_3 pastes, and ultrasonic cleaning. The main deposition parameters that influenced the diamond growth characteristics were microwave power, gas pressure, gas flow rate, reaction gases and their concentrations. Substrate temperature was not an independent parameter in this system. It was controlled mainly by the microwave power. Details about the substrate preparation and the deposition conditions are given in corresponding sections. To understand the effect of each parameter on the growth characteristics of the diamond, a series of experiments were conducted by changing only one parameter in each deposition process while other parameters were fixed at their typical values that will be given in a later section.

The deposits were characterised by a Renishaw 2000 Raman spectroscopy system and by a Hitachi 4100 scanning electronic microscope (SEM). The Raman system uses a 633 nm He-Ne laser. At this wavelength the Raman spectra of non-diamond phases of carbon are enhanced because of a resonance effect, in which the non-diamond forms of carbon scatter more effectively than diamond at longer excitation wavelength. The micro-Raman spectral resolution is 1 cm^{-1}.

To prepare a buffer layer, the copper substrates were first polished with a sequence of SiC sand papers down to 600 grid. Then they were ultrasonically cleaned in acetone for 20 min. Finally, a titanium layer approx. 2 μm thick was applied by DC sputtering. Adhesion of the diamond coating was evaluated by pull-off tests using a SHIMADZU AGS-5KND tension/compression tester. An epoxy cement was used to bond a cylindrical metal stud of 3 mm in diameter to the sample surface. The metal stud was held by a fixed clamp, and the sample by another one that was driven by a motor and could move up and down at a constant speed. The pulling force was normal to the sample surface and was recorded automatically by a computer during the test.

3. Results and discussion

3.1. Effect of substrate pre-treatment on diamond nucleation

In the investigation of the substrate pre-treatment effect, the deposition conditions were fixed as follows, if not otherwise stated: microwave power, 2500 W; gas pressure, 80 Torr; H_2 flow rate, 478 sccm; CH_4 flow rate, 30 sccm; O_2 flow rate, 1 sccm; deposition time, 30 min. All the substrates were first polished with a sequence of SiC sand papers down to 2400 grid and then pretreated differently. Ultrasonic cleaning was performed in ethanol.

3.1.1. Effect of polishing duration

The copper substrates were polished with 1 μm diamond paste for 0.5–15 min followed by an ultrasonic cleaning for 3 min. It was found that the nucleation density increased with increasing the polishing time as shown in Fig. 1. However the increase is non-linear, indicating a saturation effect for times above 10 min.

3.1.2. Effect of particle size and polishing materials

The copper substrates were polished with 0.25–15 μm diamond paste, respectively. Polishing duration was 3 min followed by a 3 min ultrasonic cleaning. Fig. 2 shows that the nucleation density increases with

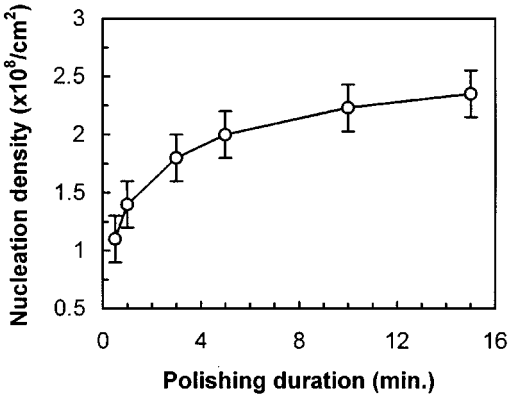

Figure 1 Nucleation density dependence on polishing duration.

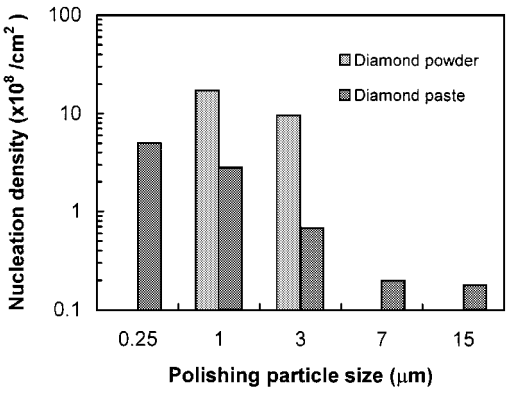

Figure 2 Nucleation density dependence on particle size in the diamond paste and diamond powder.

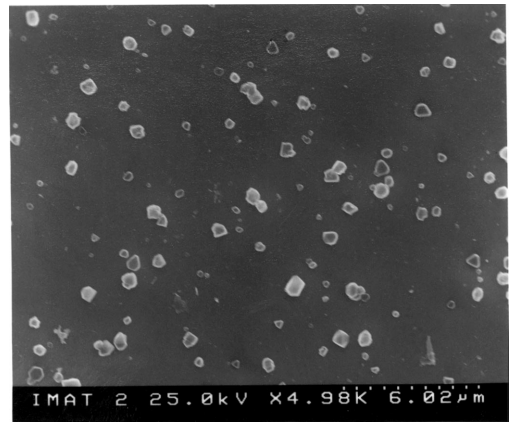

(a)

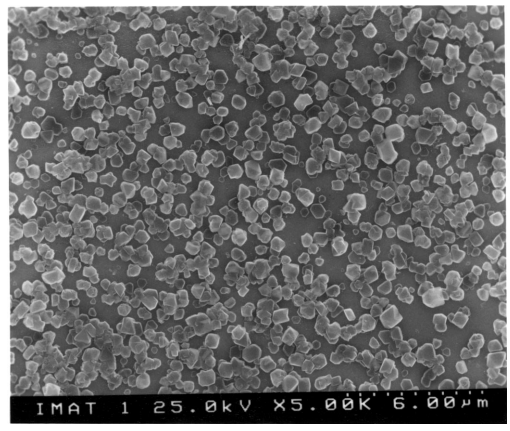

(b)

Figure 3 Diamond nucleation sites on Cu substrates polished in different sequence. (a) Sample 1: sandpaper + 7 μm diamond paste + 0.25 μm diamond paste + 0.25 μm Al_2O_3 paste. (b) Sample 2: sandpaper + 3 μm Al_2O_3 paste + 0.25 μm Al_2O_3 paste + 0.25 μm diamond paste.

decrease in size of the diamond particles in the pastes. The same tendency was found when the diamond paste was replaced by diamond powder (see Fig. 2). However, polishing with diamond powder resulted in a relatively higher nucleation density.

As a comparison, the copper substrates were polished with Al_2O_3 pastes down to 0.25 μm. The nucleation density on these samples was about 2 orders of magnitude lower than on those polished with 0.25 μm diamond paste. In addition, the nucleation sites on samples polished with only the sandpaper were very few.

Two different polishing sequences were also performed. In the first sequence (sample 1) the substrate was polished with 7 μm diamond paste, 0.25 μm diamond paste and finally with 0.25 μm Al_2O_3 paste. In the second sequence (sample 2) the substrate was polished with 3 μm Al_2O_3 paste, 0.25 μm Al_2O_3 paste and finally with 0.25 μm diamond paste. Polishing duration for each sample was 3 min for the first two steps and 0.5 min for the final step. An ultrasonic cleaning for 3 min was performed after each polishing step. Fig. 3 shows that the nucleation density on sample 1 is much lower than on sample 2.

3.1.3. Effect of ultrasonic cleaning duration after polishing

The copper substrates were polished with 7 μm diamond paste for 3 min and ultrasonically cleaned in ethanol for 3 min. Then they were polished with 1 μm diamond paste for 3 min and ultrasonically cleaned for 3-90 min. A small decrease in nucleation density with increase in the ultrasonic cleaning time was noted. For example, ultrasonic cleaning for 3 min resulted in a nucleation density of approx. $1.8\times10^8/\text{cm}^2$, while the nucleation density was still as high as about $1.4\times10^8/\text{cm}^2$ after an ultrasonic cleaning for 90 min. On samples ultrasonically cleaned for 5 min no large remains from polishing materials were found. This time of ultrasonic cleaning therefore seems to be sufficient.

3.1.4. Summary

In view of these pre-treatment results, we see that the residues from the polishing process play an important role in the diamond nucleation on copper. Fig. 3 gives strong support to this idea. For sample 1 shown in Fig. 3a, the final Al_2O_3 paste polishing removed much of the diamond residue left in the copper surface from previous polishing steps. So the nucleation density decreased. On the contrary, a reverse polishing sequence, that is, Al_2O_3 paste polishing followed by diamond paste polishing, leads to much higher nucleation density (Fig. 3b). This experiment is also in agreement with those found on Si substrate [11].

Smaller diamond particle size in polishing materials, longer polishing duration, and/or using diamond

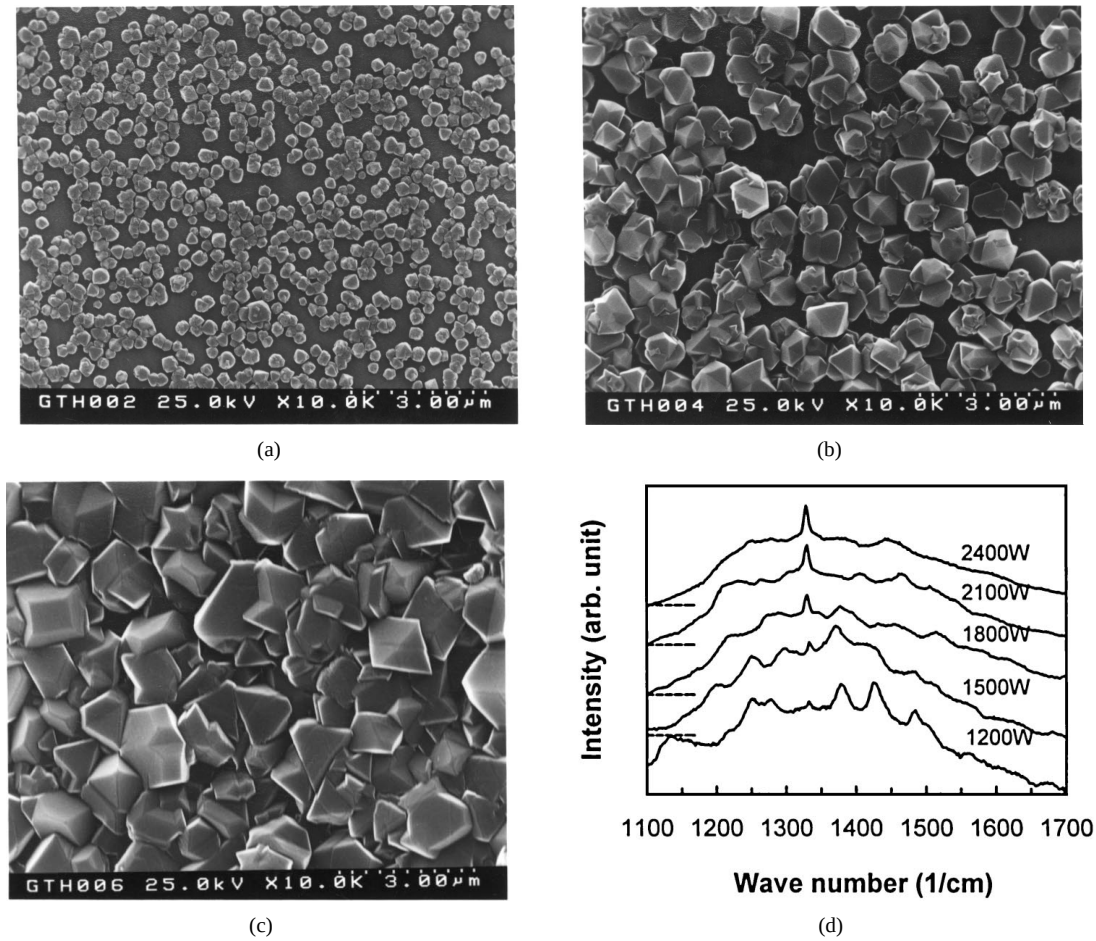

Figure 4 SEM images of diamonds synthesized at different microwave power (a) 1500 W, (b) 1800 W, (c) 2400 W, and their Raman spectra (d) with shifted base lines as indicated.

powder result in higher nucleation density as a result of higher residue density.

Ultrasonic cleaning did not affect strongly the nucleation density. In fact, copper is a relatively soft material and the diamond residues could be "seeded" into the copper surface during polishing. So, ultrasonic cleaning does not remove these residues efficiently.

According to these experimental results, we may consider the optimized pre-treatment conditions as follows: polishing time, 3∼5 min; ultrasonic cleaning time, 5 min; polishing material, diamond powder 0∼1 μm or 2∼4 μm, diamond paste 0.25 μm or 1 μm.

3.2. Effect of deposition parameters on diamond growth

In the investigation of the deposition parameter effect, typical deposition conditions were chosen according to our preliminary work, aiming at depositing diamond on Cu at low substrate temperature. They are: microwave power, 1800 W; $CH_4/(H_2 + CH_4)$, 5.9% (30 sccm/509 sccm); gas pressure, 80 Torr; gas flow rate, 509 sccm; deposition time, 85 min. The effect of each deposition parameter was studied by changing only one parameter in each experiment, while other parameters were fixed at the typical values. The substrates were polished with a sequence of sandpapers and diamond pastes down to 1 μm and optimized pre-treatment conditions as discussed above were used.

3.2.1. Effect of microwave power and substrate temperature

Microwave power was found to be the essential parameter that influenced diamond growth on Cu. Fig. 4 shows SEM images of the deposits synthesized at microwave power from 1500 W to 2400 W and their Raman spectra. The conditions for the growth of the diamond shown in Fig. 4b are for purpose of reference considered as the typical conditions. It is used to compare the effects of other deposition parameters in the following sections. It can be seen from Fig. 4 that the diamond growth rate increases with the microwave power and an evident increase in the growth rate appears when the microwave power changes from 1500 W to 1800 W. The Raman spectra (Fig. 4d) show that the intensity of the diamond peak at about 1332 cm^{-1} increases with increase in the microwave power, implying an increase in diamond phase. When the microwave power is lower than 1500 W, the formation of diamond becomes much less obvious. Instead, many amorphous components are formed. This behaviour is quite similar to the effect of substrate temperature [12] and suggests that the effect of microwave power in our experimental range is comparable to the effect of substrate temperature.

The increase in the microwave power has two concomitant effects. First, the gas temperature increases as a result of the redistribution of microwave energy transferred by the electrons, leading to an increase in the substrate temperature. Second, the plasma status

(i.e. the degree of dissociation and ionisation of H_2, CH_4 gases, electron temperature, the type and concentration of carbon-containing radicals etc.) changes. To distinguish the effects of these two factors, an additional experiment was conducted with two different Cu substrates in a same deposition process. The first substrate (1 mm thick) was put directly on the Mo sample holder as in most of the cases. The second substrate, 0.5 mm thick, was put on another 0.5 mm thick copper chip placed on the Mo holder so that heat conduction was hindered by the interface between the two chips. However, the two samples had the same height relative to the plasma. The microwave power was set at a relatively low level, 1500 W, and other parameters were set at their typical values. Much higher substrate temperature on the second sample was achieved as it appeared red, while the other one appeared grey during the deposition. On the other hand, as the height of the two samples was the same and they were put at symmetrical positions, the plasma status surrounding the first sample should be identical to that of the second one. Fig. 5 shows a SEM image of the second sample. The comparison of Fig. 5 and Fig. 4a, in which the only difference was the substrate temperature, confirms that it is the substrate temperature that governs the diamond growth.

3.2.2. Effect of methane concentration

Diamonds were deposited at different methane concentrations, but with other deposition parameters fixed at the typical values. It was found that when the methane concentration increased from 3.9% (20 sccm) to 7.8% (40 sccm), both diamond growth rate and nucleation increased. Fig. 6 shows SEM images and Raman spectra of these diamonds. The increase in the full width at half-maximum (FWHM) of the diamond Raman peak with methane concentration is to be expected as more carbon-containing radicals can be generated, while the etching effect of atomic hydrogen may become relatively insufficient, favouring the appearance of growth defects. The defects usually cause growth stresses, which are randomly oriented in all directions in the diamond films. These randomly oriented stresses can result in the broadening of the diamond Raman peak.

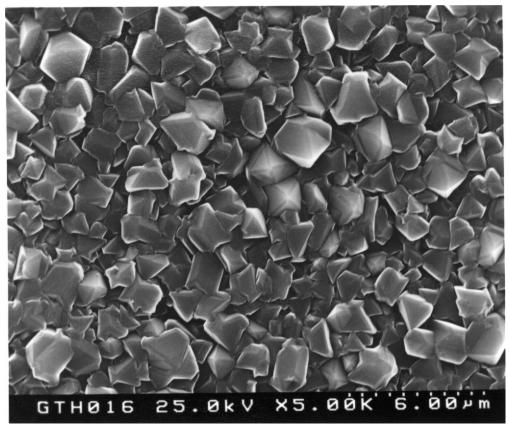

Figure 5 SEM image of diamond synthesized at microwave power 1500 W but with higher substrate temperature than that of Fig. 4a.

Also more non-diamond phases are a consequence of higher methane concentration, as can be seen from the appearance of broad peaks in the Raman spectra in Fig. 6d. The intensity of the diamond peak does not change obviously when the methane concentration changes.

3.2.3. Effect of gas pressure

Diamonds were deposited at different gas pressures, but with other deposition parameters fixed at the typical values. It was found that when the gas pressure changed from 70 Torr to 100 Torr, the diamond growth rate increased, showing an effect comparable to the methane concentration. However the increase in the diamond grain size was more obvious than the increase in the nucleation density when higher gas pressure was used. SEM images and Raman spectra of the diamonds are shown in Fig. 7. With increase in the gas pressure more diamond phase is observed, as shown by the higher intensity of the diamond Raman line. The main effect of increasing gas pressure is that the mean free path (MFP) of electrons and gas molecules decreases. As a result, the probability of interaction of electrons and molecules is higher and therefore more atomic hydrogen and carbon-containing radicals are generated. Thus, the growth rate increases with the pressure. However, when the gas pressure increases to about 100 Torr, the FWHM of the diamond peak becomes wider. This is probably due to the generation of more carbon-containing radicals as compared to atomic hydrogen. This causes an increase in the growth defects and consequently the peak broadening as discussed above.

3.2.4. Effect of gas flow rate

Diamonds were deposited at different gas flow rates (from 194 sccm to 820 sccm), but with other deposition parameters fixed at the typical values. It was found that within the gas flow rate range, the diamond grain size nearly did not change and the growth rate seemed constant, as shown in Fig. 8. Raman spectra taken from the deposits were similar to that deposited under typical conditions. When the gas flow rate changed from 194 sccm to 509 sccm, the diamond nucleation density increased slightly. However, further increasing the gas flow rate did not cause observable change in the nucleation density. We deduce that the diamond growth is mainly governed by the gas temperature and the density of reactants, which are controlled by the microwave power, gas pressure and gas concentration. Since the gas flow rate has little influence on the reactant composition and gas temperature, the diamond growth rate appears constant. On the other hand, Celii *et al.* reported that varying the gas flow rate could change both the flow pattern in the reaction chamber, especially near the substrate surface, and the ratio of convective and diffusive velocity of the reactants [13]. These factors may influence the diamond nucleation and growth, but not obviously.

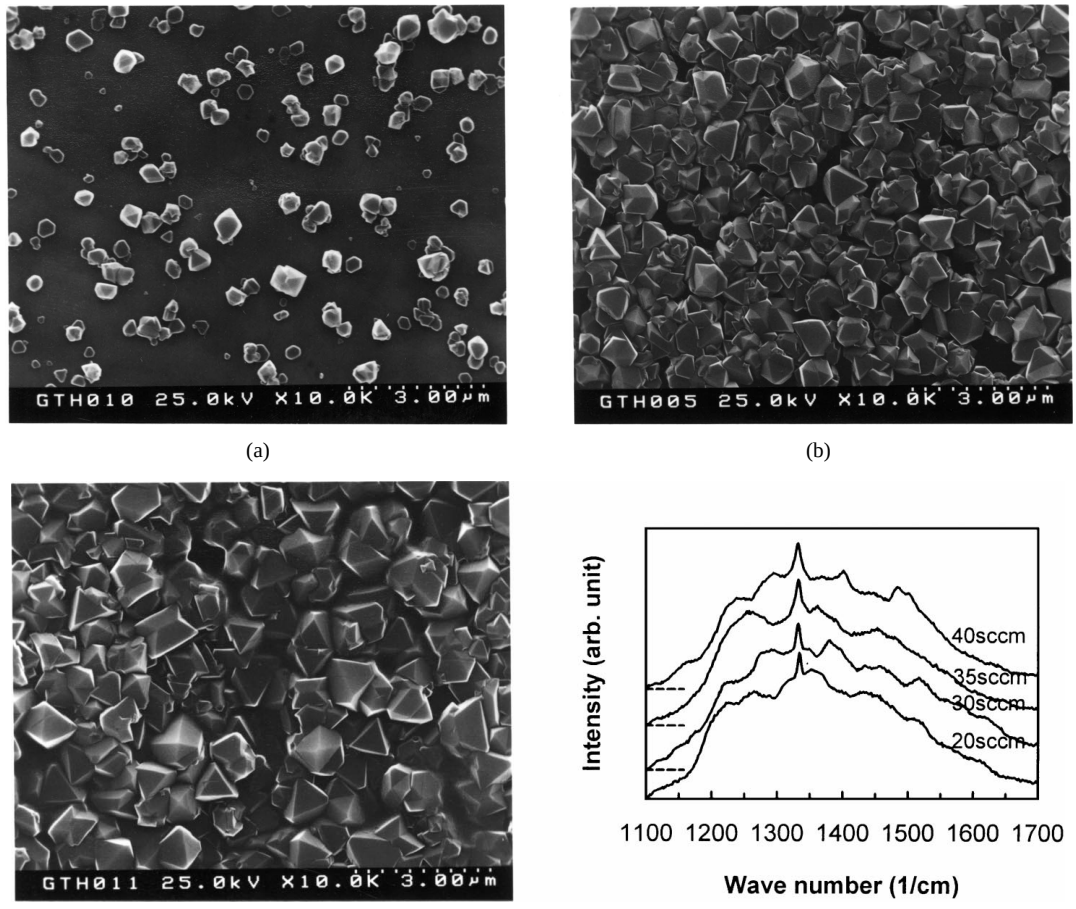

Figure 6 SEM images of diamonds synthesized at CH_4 concentration (a) 3.9% (20 sccm), (b) 6.9% (35 sccm), (c) 7.9% (40 sccm), and their Raman spectra (d) with shifted base lines as indicated.

3.2.5. Film morphology

Within our experimental range of gas pressure (70∼100 Torr), methane concentration (3.9∼7.8%), gas flow rate (193∼820 sccm), and microwave power (1200∼2400 W), the morphology of the synthetic diamonds does not show obvious change. A triangular (111) face dominating is found in almost all the cases. However, when the substrate temperature becomes high (see Fig. 4c), (100) faces appear. This is in accordance with the reports of Matsumoto *et al*. [14], Lu *et al*. [15], and Badzian *et al*. [16], who observed a dominating (111) face at lower Si substrate temperature and (100) at higher temperature.

3.2.6. Summary

Deposition parameters influence diamond growth on copper. The following growth behaviours are observed in our experimental parameter ranges.

(1) Diamond growth rate increases with increase in the microwave power and the effect of the microwave power is mainly an effect of substrate temperature. (2) Diamond nucleation and growth rate increase with increase in the gas pressure and methane concentration. When the gas pressure reaches a certain value (in our case, 100 Torr), the growth stress becomes pronounced. Increasing methane concentration results in monotonic increase in both the growth stress and non-diamond carbon phases. (3) Gas flow rate has little influence on the diamond growth. (4) The diamond crystals show a (111) face dominating in almost all the cases. Some (100) faces appear at higher microwave power (higher substrate temperature).

3.3. Free-standing diamond film preparation using copper substrate

On the base of the above pre-treatment and parametrical investigation, we tried to prepare free-standing diamond films using copper substrates, which were about 10×10 mm^2. Before deposition the substrates were polished with a sequence of SiC sandpapers and diamond pastes down to a final 1 μm. Each polishing step was about 5 min followed by an ultrasonic cleaning for 5 min.

3.3.1. Direct growth of diamond film on copper

First, diamond films were directly deposited on Cu under conditions given as follows: microwave power, 1800 W; gas pressure, 80 Torr; H_2 flow rate, 479 sccm; CH_4 flow rate, 30 sccm; O_2 flow rate, 1 sccm. The substrate temperature was about 600 °C. By changing the deposition time, films with different thickness were obtained. During the post cooling procedure after deposition, different cracking behaviours were observed. When the films were thinner than 15 μm, they

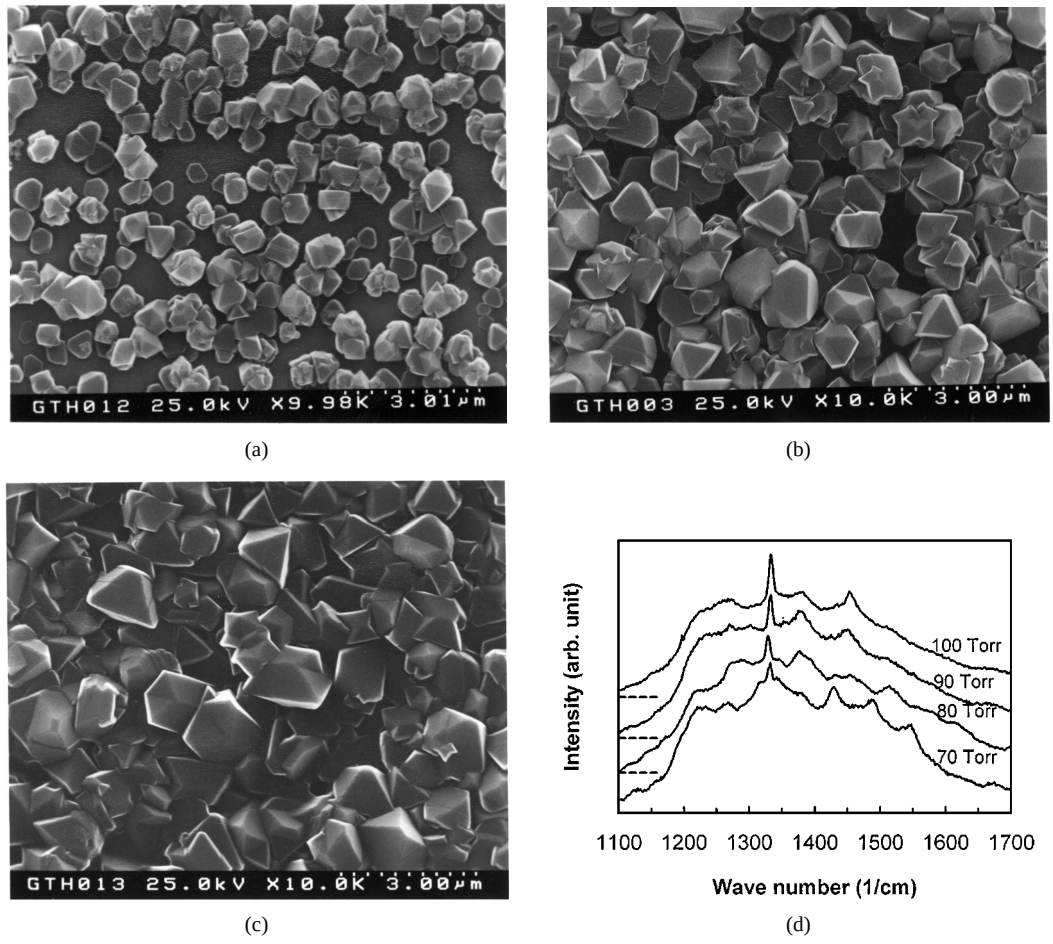

Figure 7 SEM images of diamonds synthesized at gas pressure (a) 70 Torr, (b) 90 Torr, (c) 100 Torr, and their Raman spectra (d) with shifted base lines as indicated.

usually cracked. However, no cracking happened in films thicker than 20 μm.

If the films had no adhesion and just attached loosely to the Cu substrate surface during post cooling procedure, they would not crack upon thermal contraction of the Cu substrate. Since Cu does not form carbide, the adhesion and attachment most probably come from two main aspects. One is the roughness of the Cu surface, which can be improved by the polishing process, but could not be eliminated completely. The other is impurities in the Cu and the residues seeded in the Cu surface after the polishing process. Actually, our previous results in part 3.1 showed that these residues could greatly enhance diamond nucleation, suggesting that many diamond grains grow up on these residues. Thus, during the post cooling procedure, because of the thermal mismatch between the Cu substrate and the diamond film as well as above mentioned two reasons, a thermal stress may apply to the film. This stress can be expressed as

$$\sigma_{\text{th}} = \frac{E}{1-\nu}\int_{T_s}^{T_d}(\alpha_f - \alpha_s)dt \qquad (1)$$

where $E = 1143$ GPa and $\nu = 0.07$ are Young's modulus and Poisson's ratio for diamond [17]. T_d and T_s are deposition temperature and sample temperature during cooling procedure. α_f and α_s are temperature-dependent thermal expansion coefficients of diamond film and copper, and can be found in [18] and [19], respectively. Assuming $T_d = 600\,^{\circ}$C and $T_s = 25\,^{\circ}$C (room temperature), we conducted a numerical calculation of Equation 1 and obtained a compressive thermal stress $\sigma_{\text{th}} \approx -8.78$ GPa.

It can be seen that σ_{th} increases with decrease in T_s, which implies that during the post cooling procedure, thermal stress in the diamond film increases. If the diamond grains are trapped at the Cu surface and cannot be released during the cooling procedure, then the whole thermal stress σ_{th} applies to the film. This can cause film cracking if the strength of the film is not enough to support the thermal stress σ_{th}. On the other hand, if the grains are released from the trapped positions at a point during post cooling when the film strength is still large enough, then no cracking is expected. So, it is the relative strength of the diamond film and the thermal stress σ_{th} needed to release the diamond grains from their trapped positions that determines if the diamond film cracks. Obviously, the film strength increases with the film thickness. This could be the main reason that thicker films are unlikely to crack.

3.3.2. Two-step growth for stress relief

From the above discussion we can see that there are several possible ways to avoid film cracking. First, by decreasing the deposition temperature T_d so as to reduce

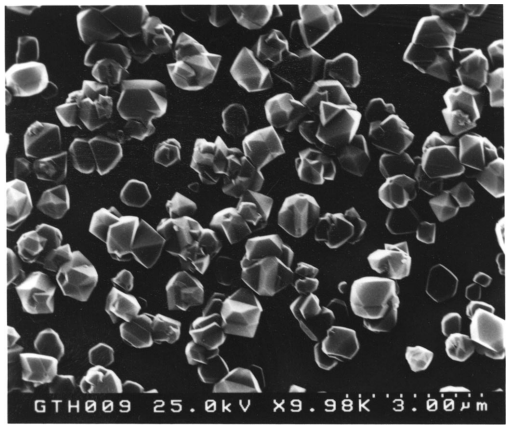

(a)

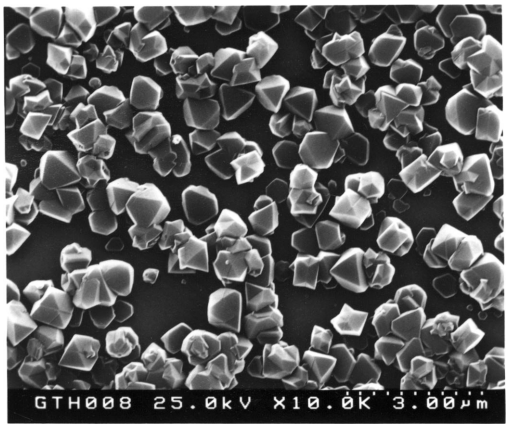

(b)

Figure 8 SEM images of diamonds synthesized at gas flow rate (a) 194 sccm, (b) 820 sccm.

the thermal stress σ_{th}. However, this may cause a low film growth rate due to the low substrate temperature as shown in part 3.2. Second, by increasing the film strength, i.e., the film thickness. This has been verified by our experiments. Third, by releasing the diamond grains from the Cu surface before the film cracking happens. Based on the third idea, we propose a two-step growth method. This method includes a pre-growth, during which a short deposition is performed to obtain a quasi-continuous diamond on Cu substrate; a quick rampdown which allows many of the diamond grains to be released from their trapped positions; and a final growth stage characterized by a longer deposition at a slightly lower microwave power level. The optimized deposition conditions for these two stages are shown in Table I. Relatively thin free-standing diamond films ($\sim$10 μm) are prepared with this method.

Fig. 9 shows the diamond grown on Cu after the first growth stage. As the deposits are not continuous

TABLE I Deposition conditions of the two growth stages

Deposition parameter	Stage 1	Stage 2
Microwave power (W)	2000	1800
Gas pressure (Torr)	90	85
H_2 flow rate (sccm)	478	478
CH_4 flow rate (sccm)	35	30
O_2 flow rate (sccm)	1	1
Growth time (h)	0.25	12

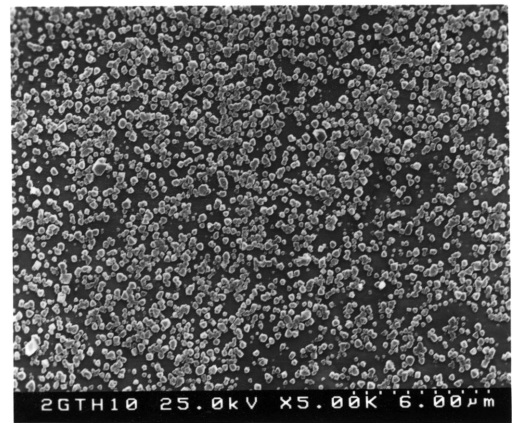

Figure 9 Diamond grown on Cu after the first deposition stage of the two-step growth.

yet, there is no visible cracking. This means that the grains are just slightly released from the Cu surface due to the quick rampdown following the first growth step. Our investigation shows that the control of the first growth stage is critical. If the growth time is too short, the nucleation will not be sufficient. This may cause new nucleation during the final growth stage and consequently the film cracks as a result of insufficient releasing of the grains from the Cu surface. On the other hand, if the growth time is too long, the deposits will be continuous and cracking happens even just after the first growth stage.

After the final growth, a sufficiently flat and relatively thin film ($\sim$10 μm) in an area of 10 $\times$ 10 mm^2 is obtained without cracking. The film can be easily removed from the copper substrate and becomes free-standing. Fig. 10 shows SEM images of the surface and back side of the free-standing diamond film prepared by this two-step growth method and their Raman spectra. It can be seen that the grain size at the film back side is much smaller than at the surface side. This is because once the first nucleation particles grow up and meet each other, they can no longer grow in the Cu surface plane but can continue to grow in a perpendicular direction. As a result of growth competition, some preferential grains become larger and larger until they reach an equilibrium. The Raman spectra show a sharp peak at about 1332 cm^{-1}, indicating the existence of good quality diamond phase. No carbide transition layer is found, as expected. The background of the Raman spectrum of the film back side is obviously higher than that of the surface side, although the diamond peak presents similar width and position. Thus the background in the back side may arise mainly from the grain boundaries, as the grain size in this side is much smaller.

3.3.3. Summary

Our investigation shows that free-standing diamond films can be prepared using Cu substrate by CVD. Relatively thin films ($\sim$10 μm) are obtained using a two-step growth method for stress relief. Thicker films ($>$20 μm) can be prepared through direct deposition. The free-standing diamond films grown on Cu show uniform diamond phase at the film surface side and

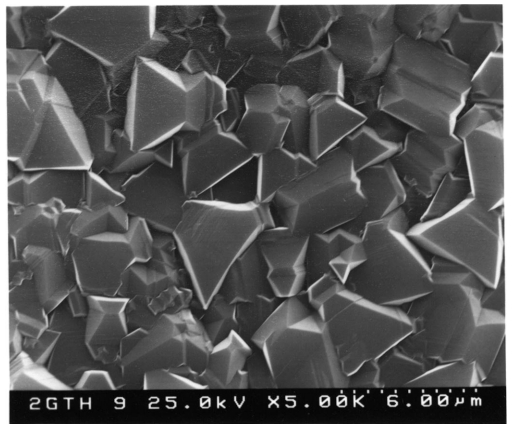

(a)

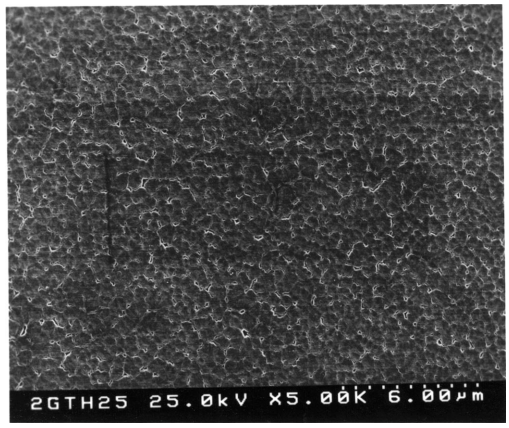

(b)

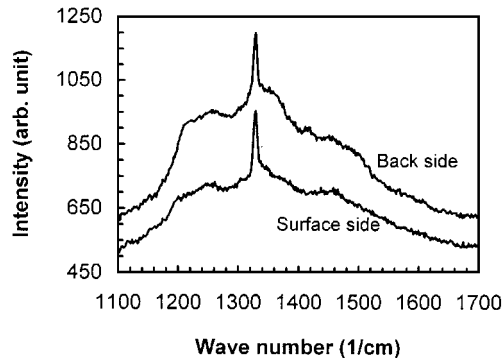

(c)

Figure 10 SEM images and Raman spectra of the free-standing diamond film prepared by the two-step growth method. (a) film surface side, (b) film back side, (c) Raman spectra taken from the two sides under identical conditions.

back side. There is no carbide transition layer at the interface of the substrate and the diamond film as Cu has no carbon affinity.

3.4. Effect of the titanium interlayer

To obtain adherent diamond coating on copper, a titanium interlayer was used. The reason for choosing titanium is that it forms carbide and has a reasonable diffusibility in copper. So, it is expected that titanium can provide good adhesion to both the diamond film and the copper substrate. Before deposition, the substrates were scratched with 3 μm diamond powder for 1 min and then ultrasonically cleaned in ethanol for 3 min. Diamond films were grown under conditions

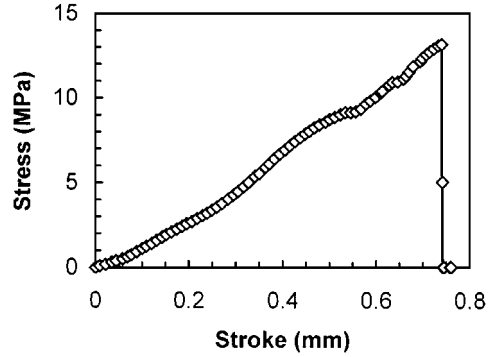

Figure 11 Pull-off test result showing the critical detaching force. Note that the detachment happens at the diamond film/epoxy glue interface, indicating the adhesion of the diamond coating is better than the epoxy.

given as follows: microwave power, 1800∼2400 W; gas pressure, 80 Torr; H_2 flow rate, 475 sccm; CH_4 flow rate, 25 sccm. The substrate temperature, mainly controlled by the microwave power, was within the range of 500∼800 °C.

Pull-off tests were conducted using samples coated at different microwave power from 1800 W to 2400 W. All the tests showed that the debonding happened between the diamond film and the epoxy glue, indicating that the adhesion of the diamond films to the substrates was stronger than the epoxy. Fig. 11 shows a typical result of the pull-off test on a sample coated at 2400 W microwave power. It can be seen that the critical detaching force *between the epoxy and the diamond film* is about 14 MPa. So, we conclude that with the titanium interlayer, adherent diamond film can be coated on copper.

Fig. 12 shows SEM images of diamond films grown on the titanium coated copper substrate at different microwave powers. It can be clearly seen that the grain size increases with the microwave power. This can be explained as a result of the increase in the diamond growth rate with the substrate temperature. However, the morphology of these diamond films does not show obvious change. A triangular (111) face dominating is observed in all the cases. These results are similar to those mentioned in section 3.2.1, though in the two cases the substrates are different (Ti/Cu and Cu). This implies that the diamond growth characteristics are mainly controlled by the deposition conditions.

It has been known that residual stresses usually affect the film adhesion in a negative way. So, it is significant to understand how the deposition process influences the residual stresses in the diamond films. As mentioned before, thermal mismatch between the diamond film and the copper substrate is very large, which may cause large residual stress. Thus, we mainly investigate the effect of deposition temperature on the residual stress in the diamond films. Three samples were deposited at different microwave powers of 1800 W, 2100 W, 2400 W for 22.5 h, 13.5 h, and 6 h, respectively. The use of different deposition times was aimed at obtaining similar film thickness. The thickness of these films was about 16 μm. The diamond Raman peak shifted from its normal position, 1332 cm^{-1}, to higher wave numbers with increase in the microwave power, as shown in

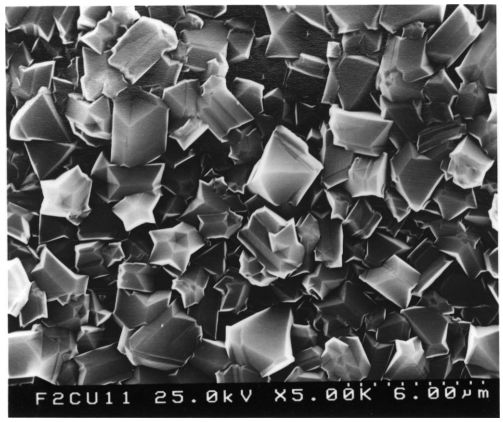

(a)

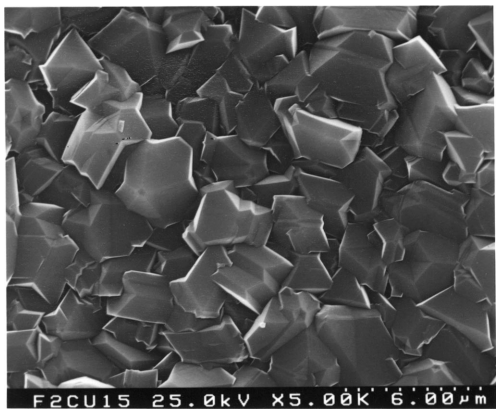

(b)

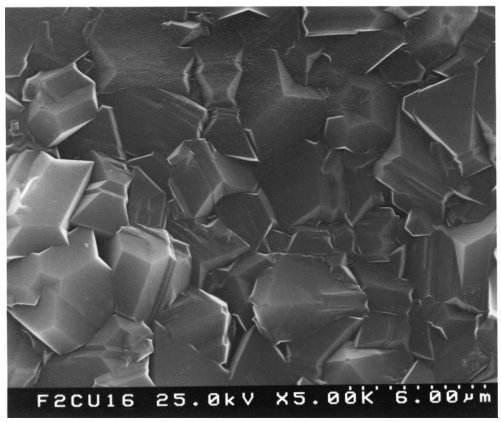

(c)

Figure 12 SEM images of the diamond films grown for 8 h on the Ti coated copper substrate at microwave power (a) 1800 W, (b) 2100 W, and (c) 2400 W.

Fig. 13. As a comparison, diamond films were also deposited on copper substrates without the titanium layer in the same deposition processes at 1800 W, 2100 W, and 2400 W microwave power. In this case, the diamond films had no adhesion to the copper substrates. Raman spectra taken from these films did not show an observable shift in the diamond peak position (Fig. 13).

The shift of the diamond Raman peak to higher wave numbers has been attributed to a compressive stress [20–21], which is believed to be caused mainly by a mismatch in thermal expansion coefficients of the diamond film and the substrate. According to the shift, the stress in the diamond film can be evaluated. Ager and Drory have shown that under a biaxial stress σ the Raman line of polycrystalline diamond splits into a

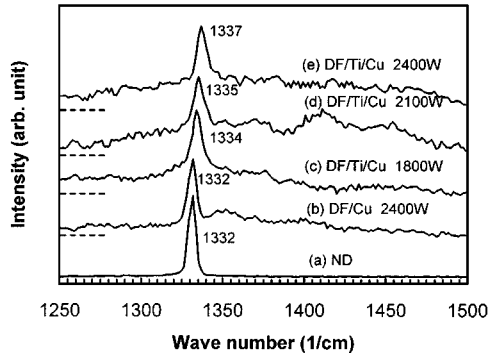

Figure 13 Raman spectra taken from natural diamond ((a) ND), diamond film grown on copper at 2400 W microwave power for 6 h ((b) DF/Cu 2400 W), diamond films grown on Ti coated copper substrates at microwave power 1800 W for 22.5 h ((c) DF/Ti/Cu 1800 W), 2100 W for 13.5 h ((d) DF/Ti/Cu 2100 W), 2400 W for 6 h ((e) DF/Ti/Cu 2400 W).

singlet and a doublet [21]. They shift from the normal 1332 cm^{-1} position by $\Delta\tau_s$ (singlet) and $\Delta\tau_d$ (doublet), respectively. Relationship between the stress and the shifts can be expressed as

$$\sigma(\mathrm{GPa}) = -1.08\Delta\tau_s\,(\mathrm{cm}^{-1}) \quad \text{for singlet,} \qquad (2)$$

and

$$\sigma(\mathrm{GPa}) = -0.384\Delta\tau_d\,(\mathrm{cm}^{-1}) \quad \text{for doublet.} \qquad (3)$$

Sometimes the peak splitting is not obvious. As an approximation, we may assume the measured peak shift as the centre point between the singlet and the doublet, i.e., $\Delta\tau_{\mathrm{measured}} = 0.5(\Delta\tau_s + \Delta\tau_d)$, and obtain

$$\sigma(\mathrm{GPa}) = -0.568\Delta\tau_{\mathrm{measured}}\,(\mathrm{cm}^{-1}). \qquad (4)$$

Thus, the stress in the diamond film is proportional to the Raman peak shift. From Fig. 13 we can see that the Raman shift increases with the microwave power, that as shown above in turn accounts for the substrate temperature. For example, at microwave powers of 1800 W and 2400 W, the diamond Raman peak shifts to about 1334 cm^{-1} and 1337 cm^{-1}, corresponding to a compressive stress -1.14 GPa and -2.84 GPa (Equation 4), respectively. Therefore, the stress in the film is greatly reduced at lower microwave power, i.e., lower substrate temperature.

On the other hand, the thermal stress σ_{th} in the CVD diamond film can be expressed by Equation 1. Suppose the deposition temperature T_d was relatively low, about 600 °C, and room temperature $T_s = 25$ °C, a numerical calculation of Equation 1 yields a compressive thermal stress $\sigma_{\mathrm{th}} \approx -8.78$ GPa. It is known that the stress σ in the diamond film consists of thermal stress σ_{th} and intrinsic stress σ_{in}, i.e.,

$$\sigma = \sigma_{\mathrm{th}} + \sigma_{\mathrm{in}}. \qquad (5)$$

As mentioned above, the diamond growth characteristics are mainly controlled by the deposition conditions. The fact that Raman spectra taken from the free-standing films do not show an observable shift in the

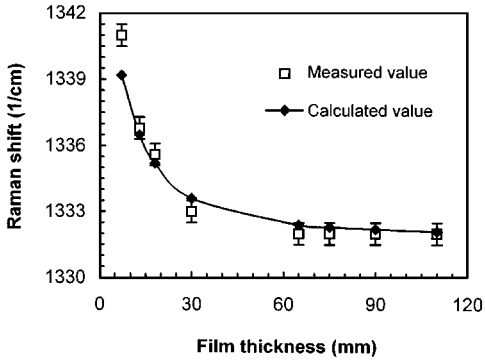

Figure 14 Experimental and calculated Raman peak shift dependence on the thickness of diamond film grown on the Ti coated copper substrate.

diamond peak position implies that the biaxial intrinsic stress σ_{in} is small. Considering that the spectral resolution is 1 cm^{-1}, a Raman shift ranging from 1331.5 to 1332.5 cm^{-1} is regarded as 1332 cm^{-1} in the measurement. Thus, the intrinsic stress σ_{in}, even though in tension, is only about 0.284 GPa at maximum (corresponding to a 0.5 cm^{-1} shift, Equation 4). According to Equation 5, the residual stress σ is still about -8.496 GPa in compression. This value is still much higher than that obtained from the shift of the diamond Raman peak, implying that the stress in the film is released.

In order to understand the stress relaxation behaviour, further experiments were conducted. Diamond films were deposited at 2100 W microwave power for different times so that different film thicknesses were obtained. Raman spectra taken from these samples exhibit different shifts of the diamond peak, as shown in Fig. 14. If we consider only the thermal mismatch, these Raman spectra should exhibit the same diamond peak shift. However, it can be seen that the thicker the film, the smaller the diamond peak shift. To explain this effect, we assume that near the substrate/diamond film interface, there is first a very stressed layer due mainly to the mismatch in thermal expansion, growth defects and lattice mismatch. With the growth of the diamond film, the stress in the surface layer gradually decreases due to the accommodation of the layers underneath. This stress relaxation leads to a difference of stress along the depth of the film. Meanwhile, due to optical absorption, the Raman signal intensities coming from different depths of the film are different. Raman spectra taken from the film are actually a superposition of a series of 'layers' (in fact, it is a continuum), that contribute differently to the observed diamond Raman peak, in both peak position and peak intensity. In our Raman measurements, no confocal components were installed and the laser beam was focused at the film surface. So, it is expected that the surface layer of the diamond film contributes to a smaller shift due to lower stress, but a higher intensity due to less absorption of the incident laser and the Raman signals. However, for deeper layers, the contribution is the contrary. Therefore, when dealing with the effect of film thickness on the diamond Raman shift, we have to consider how the stress and the Raman signal intensity change along the depth.

A simple calculation is performed in order to know the stress variation along the depth of the film. The

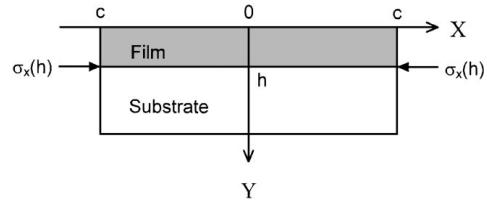

Figure 15 A configuration of the diamond film-copper substrate for the calculation reference.

configuration of the diamond coating on copper is shown in Fig. 15 for the calculation reference. We assume that at the film/substrate interface ($y = h$), there is a uniform compression $\sigma_x(h) = q$, while at the film surface ($y = 0$), the inplane stress is zero, $\sigma_x(0) = 0$, due to the free boundary. As the substrate width $2c$ is much larger than the film thickness h and the boundary stresses at $y = 0$ and $y = h$ are uniform along the x direction, we may neglect the non-uniformity of the in-plane stress near the edge of the film and suppose that the in-plane stress σ_x is uniform in the x direction. Then the Airy stress equation [22]

$$\frac{\partial^4\phi}{\partial x^4} + 2\frac{\partial^4\phi}{\partial^2 x \partial^2 y} + \frac{\partial^4\phi}{\partial y^4} \tag{6}$$

becomes

$$\frac{\partial^4\phi}{\partial y^4} = 0, \tag{7}$$

where ϕ is stress function. Solving Equation 7, we obtain the stress function

$$\phi = k_1 y^3 + k_2 y^2 + k_3 y + k_4, \tag{8}$$

where k_1, k_2, k_3, k_4 are constants to be determined. The in-plane stress σ_x can be deduced from the stress function ϕ

$$\sigma_x = \frac{\partial^2\phi}{\partial y^2}. \tag{9}$$

Using boundary conditions mentioned above, i.e., $\sigma_x(0) = 0$ for $y = 0$, $\sigma_x(h) = q$ for $y = h$, we find

$$\sigma_x = \frac{q}{h} y. \tag{10}$$

Equation 10 shows that the stress in the film changes linearly along the depth of the film. Thus, combining Equation 10 and Equation 4, we can obtain the Raman shift τ contributed by a layer at depth y of the film

$$\tau = 1332 - \frac{1}{0.568}\frac{q}{h} y \ (\mathrm{cm}^{-1}). \tag{11}$$

It should be noted that q is negative for compressive stress and positive for tension stress.

On the other hand, the absorption loss δI is in proportion to the thickness δy of a material that the electromagnetic wave penetrates

$$\delta I = -\eta I \delta y, \tag{12}$$

where η is loss factor, I the signal intensity at depth y. Here, the loss factor η includes the intensity loss of both the incident light and the Raman signal. Its value depends on the material and its structure as well as the laser source. According to Equation 12, we find

$$I = I_0 e^{-\eta y}, \tag{13}$$

where I_0 is the intensity of Raman signal coming from the surface layer. Equation 13 implies that the intensity of the Raman signal contributed by different layers decreases exponentially along the depth of the film.

Using a Lorentzian function to simulate the Raman spectra of different 'layers', we find

$$I_y = \frac{I_0 e^{-\eta y} \omega^2}{(\lambda - \tau)^2 + \omega^2} \tag{14}$$

where I_y is the intensity of the Raman signal coming from a depth of y microns, ω the full width at half-maximum (FWHM), λ the wave numbers, τ the peak centre that can be obtained from Equation 11. Then the total intensity I_t is a summary of all I_y

$$I_t = \sum I_y. \tag{15}$$

As an approximation, we imagine dividing the film into layers with a 1 micron step, and in each layer the stress and the Raman signal intensity are constants. Assuming the loss factor $\eta = 0.1$, and the FWHM $\omega = 6\,\mathrm{cm}^{-1}$, we obtain the simulated Raman spectra, i.e., I_t–λ curves. One example is shown in Fig. 16. In this case, the film is 13 μm in thickness. The simulated Raman shift is 1336 cm^{-1}, which is in agreement with the experimental value. As a comparison, the simulated Raman shifts for different film thicknesses are also given in Fig. 14. The calculated results agree with the experimental results except for a small deviation at lower thicknesses, probably due to that during the growth of the diamond film, its structure, such as grain size and grain boundary, changes significantly, causing a non-uniformity of the film. At lower thickness the grains are smaller and denser, thus the stress relaxation is no longer so effective as described by the model above; i.e., the actual stress can be larger than that given by Equation 10. According to the above discussion, we suggest that the stress relaxation along the depth of the diamond film is an important contributor to the disagreement in stress evaluation from the diamond Raman peak shift and the thermal mismatch.

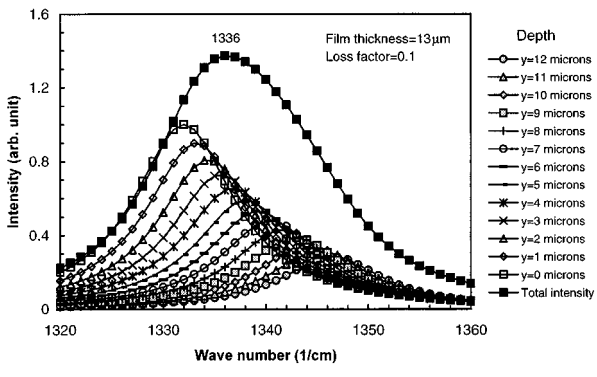

Figure 16 An example of a simulated diamond Raman spectrum. The thickness of the diamond film is 13 μm. The FWHM ω of the spectrum of each layer and the loss factor η are assumed 6 cm^{-1} and 0.1, respectively.

4. Conclusions

1) Diamond nucleation on copper is strongly affected by substrate pre-treatment. Smaller diamond particle size in polishing materials and/or longer polishing duration result in higher nucleation density. Ultrasonic cleaning does not affect the nucleation density significantly because copper is a relatively soft material and the residues can be "seeded" in the copper surface. The fact that diamond polishing followed by Al_2O_3 paste polishing greatly reduces the nucleation density supports the idea that the residues left in the copper substrate surface play an important role in diamond nucleation.

2) Deposition parameters control the diamond growth characteristics. The diamond growth rate increases with microwave power and gas pressure. Increasing methane concentration leads to the increase in nucleation and growth rate at the cost of sacrificing diamond quality. Gas flow rate has little influence on the growth rate.

3) Relatively thick free-standing diamond films (>20 μm) can be prepared directly using copper substrates, while thinner films ($\sim$10 μm) can be prepared by a two-step growth method which may effectively release the thermal stress.

4) Using a titanium interlayer, diamond films have been coated on ordinary copper. Pull-off tests show that the adhesion of the diamond film to the substrate is better than 14 MPa. Lower deposition temperature leads to lower residual in-plane stress in the diamond film. The residual stress evaluated from the shift of the diamond Raman line is usually smaller than that evaluated from the mismatch in thermal expansion coefficients of diamond film and copper. Therefore, the stress relaxation along the depth of the diamond film should be taken into account.

Acknowledgements

The authors would like to thank Mr. A. Fernandes for his help in experiments. NATO research project SFS-PO-OPTOELECT is acknowledged. One of the authors, Q. H. Fan, would like to thank JNICT (Portugal) for financial support.

References

1. M. N. R. ASHFOLD, P. W. MAY, C. A. REGO and N. M. EVERITT, *Chemical Society Review* **21** (1994) 23.
2. J. NARAYAN, V. P. GODBOLE, G. MATERA and R. K. SINGH, *J. Appl. Phys.* **71** (1992) 966.
3. T. P. ONG, F. XIONG, R. P. H. CHANG and C. W. WHITE, *J. Mater. Res.* **7** (1992) 2429.
4. R. RAMESHAM, F. M. ROSE and A. ALLERMAN, *Diamond Relat. Mater.* **1** (1992) 907.
5. S. I. OJIKA, S. YAMASHITA, K. KATAOKA and T. ISHIKURA, *Jpn. J. Appl. Phys.* Part 2, **32** (1993) L1681.

6. S. D. WOLTER, B. R. STONER and J. T. GLASS, *Diamond Relat. Mater*. **3** (1994) 1188.
7. M. L. HARTSELL and L. S. PLANO, *J. Mater. Res*. **9** (1994) 921.
8. E. PEREIRA, QI HUA FAN and J. J. GRACIO, *Mater. Res. Soc. Symp. Proc*. **436** (1996) 323.
9. M. ECE, B. ORAL and J. PATSCHEIDER, *Diamond Relat. Mater*. **5** (1996) 211.
10. QI HUA FAN, J. GRACIO and E. PEREIRA, *Diamond Relat. Mater*. **6** (1997) 422.
11. E. J. BIENK and S. ESKILDSEN, *Diamond and Relat. Mater*. **2** (1993) 432.
12. Y. MURANAKA, H. YAMASHITA and H. MIYADERA, *Diamond Relat. Mater*. **3** (1994) 313.
13. F. G. CELII, D. WHITE, JR. and A. J. PURDES, *J. Appl. Phys*. **70** (1991) 5636.
14. S. MATSUMOTO, Y. SATO, M. TSATSUMI and N. SETAKA, *J. Mater. Sci*. **17** (1982) 3106.
15. Z. P. LU, J. HERBERLEIN and E. PFENDER, *Plasma Chemistry and Plasma Processing* **12** (1992) 35.
16. BADZIAN, in "Synthetic Diamond: Emerging CVD Science and Technology," ed., K. E. Spear and J. P. Dismukes (Wiley-Interscience, New York, 1994) pp. 171–184 and pp. 243–299.
17. C. A. KLEIN and G. F. CARDINALE, *Diamond Relat. Mater*. **2** (1993) 918.
18. G. DAVIES, in "Properties and Growth of Diamond" (INSPEC, London, 1994) p. 25.
19. K. RAZNJEVIC, in "Handbook of Thermodynamic Tables and Charts" (Hemisphere Publishing Corporation, Washington, 1976) p. 6.
20. D. S. KNIGHT and W. B. WHITE, *J. Mater. Res*. **4** (1989) 385.
21. J. W AGER and M. D. DRORY, *Phys. Rev. B*, **48** (1993) 2601.
22. S. P. TIMOSHENKO and J. N. GOODIER, in "Theory of Elasticity" (McGraw-Hill Inc., Tokyo, 1970) p. 32.

Received 18 June
and accepted 21 August 1998